# Results of the comprehensive interpretation of well logs in carbonate and siliciclastic rocks – similarities and differences in the case studies of selected formations

Sebastian Waszkiewicz[1], Ronal Barcala Alvarez[2], Jadwiga Jarzyna[3]

[1] AGH University of Science and Technology, Faculty of Geology, Geophysics and Environmental Protection, Department of Geophysics (Ph.D. student); al. A. Mickiewicza 30, 30-059 Krakow, Poland
[2] Cuban Oil Union, Oil Research Center (CEINPET); Havana, Cuba; e-mail: ronal.b.alvarez@gmail.com
[3] AGH University of Science and Technology, Faculty of Geology, Geophysics and Environmental Protection, Department of Geophysics, al. A. Mickiewicza 30, 30-059 Krakow, Poland; e-mail: jarzyna@agh.edu.pl; ORCID ID: 0000-0002-1803-8643

*Abstract:* This paper was made using geological and well logging data from the Cuban oilfield area and the Polish Carpathian Foredeep gas deposit to compare the interpretation process and underline similarities and differences between data analysis from two reservoir rocks of different lithology. Data from conventional hydrocarbon deposits, i.e. the Mesozoic Cuban carbonate formation and Miocene shaly-sandy sediments were processed and interpreted using Techlog (Schlumberger Co.) software. Selected approaches were used to determine the step by step volume of shale, total and effective porosity, water/hydrocarbon saturation (Quanti) and for the comprehensive interpretation of well logs (Quanti Elan). Brief characteristics of the carbonate and siliciclastic formations were presented to indicate that the interpretation methodology oriented to the determination of petrophysical properties depends strongly on the type of reservoir. Cross-plots were presented for primary mineral composition recognition, determination of m exponent and resistivity of formation water in the Archie equation. Effective intervals for the carbonate reservoir were calculated according to the Cumulative Hydrocarbon Column methodology. Finally, the results of the interpretation of well logs were presented as continuous curves of mineral composition, including shaliness, porosity and hydrocarbon saturation. The conclusions included recommendations for the effective comprehensive interpretation of well logs in the carbonate and siliciclastic reservoirs.

*Keywords:* comprehensive interpretation of well logs, carbonates, siliciclastic rocks, Cuban oilfield area, Carpathian Foredeep

## INTRODUCTION

Interpretation of well logging data in various rock formations is based on the same physical principles but, because of differences in geological and reservoir conditions influencing the recorded logs, especially petrophysical parameters, the results may be dissimilar. A correct interpretation allows a reservoir and its production potential to be recognized and mistakes resulting in a large economic failure to be avoided. Determination of the reservoir parameters of selected beds is carried out through qualitative and quantitative interpretation and is heavily dependent on lithology in both cases.

Carbonate and siliciclastic formations are main goals in hydrocarbon prospecting due to their

reservoir properties, i.e. porosity and permeability characterizing hydrocarbons cumulating and producing ability. The geological construction of reservoirs is mainly related to the origin conditions which have influenced the petrophysical parameters in a specific way. The considered reservoirs differ not only in terms of mineral composition but also in the type and volume of porosity and volume and distribution of clay minerals in the rock matrix and pore space. The mentioned differences resulted in special approaches to interpretation. They led to different rock matrix models being adopted and required different equations to be employed in order to calculate shaliness, total and effective porosity, absolute, phase and relative permeability and, most importantly, water/hydrocarbons saturation, i.e. the volume of residual and movable hydrocarbons (Serra 1984, Jarzyna et al. 1999, Asquith & Krygowski 2004). The petrophysical properties obtained in well logging interpretations are important components in various geophysical and geological applications, for instance seismic modelling or recognition in details rock formation adopted for gas or $CO_2$ storage (Niepsuj & Krakowska 2012, Nosal & Semyrka 2012), so in many cases the further results depend on the accuracy of their initial determination.

Usually, the interpretation of well log data is realized in a two-step process. Firstly, there is a qualitative interpretation based on the combination/comparison of well logging traces at the proper scale. At that stage, lithology identification and bed thickness determination were made, together with the pre-selection of hydrocarbon-saturated formations. In addition, cross-plots (2D or 3D) have a wide range of applications at this stage. Constructing cross-plots means visualizing well logging data in 2D or 3D dimensions. Applying special overlays fitted to records of used logging tools and implementing cross-plots reveals even more information about a formation than a standard log vs. depth display.

The main aim of the quantitative interpretation is the determination of the volume of mineral components and calculating the reservoir parameters of the formation in question. In many computer systems used by service companies in the hydrocarbon prospecting industry (ULTRA in Halliburton Co., Quanti Elan in

Schlumberger Co., Interactive Petrophysics by Lloyd's Register and others), the inverse problem is solved on the basis of a model which combines the volume of mineral components and porosity saturated with hydrocarbons and formation water. To solve this problem, a set of linear or linearized equations is built where on the left hand side there is an outcome of well log, for instance bulk density (RHOB) and on the right – sum of products of volumes of mineral constituents selected by interpreter multiplied by specific parameters related to the physical property which is the basis of the well log (i.e. the specific density of the minerals) and porosity partially filled with formation water and hydrocarbons. In the majority of cases, error minimizing methods are applied to solve a determined or over-determined set of equations and obtain the best model fitted to the mineralogical and saturation expectations, in agreement with laboratory measurements or borehole tests. The number of equations depends on a number of unknown aspects, i.e. rock mineral components and available logs. For example, for four component model in which the unknowns are: volumes of two minerals, shale volume and porosity and measured logs are neutron, density and sonic, system of equation looks as follows (1) assuming that it refers to the flushed zone and the porosity is fully filled with mud filtrate:

$$\phi_b = V_1 \cdot \phi_{N_1} + V_2 \cdot \phi_{N_2} + V_{sh} \cdot \phi_{N_{sh}} + \phi$$

$$\rho_b = V_1 \cdot \rho_{ma1} + V_2 \cdot \rho_{ma2} + V_{sh} \cdot \rho_{sh} + \phi \cdot \rho_f \qquad (1)$$

$$DT = V_1 \cdot DT_{ma1} + V_2 \cdot DT_{ma2} + V_{sh} \cdot DT_{sh} + \phi \cdot DT_f$$

$$1 = V_1 + V_2 + V_{sh} + \phi$$

where:

$V_1, V_2, V_{sh}$ – volumes of the 1st and 2nd minerals and shale,

$\phi_{N_{1,2}}, \phi_{N_{sh}}$ – neutron porosity of the 1st and 2nd minerals and shale,

$\rho_{ma1,2}, \rho_{sh}, \rho_f$ – specific density of the 1st and 2nd minerals, shale and pore fluids,

$DT_{ma1,2}, DT_{sh}, DT_f$ – sonic travel time of the 1st and 2nd minerals, shale and pore fluids.

The last equation (balance equation):

$$1 = V_1 + V_2 + V_{sh} + \phi$$

is always present. It informs about the occurrence of individual components in the model. Then, in software using optimization algorithms, the model is fitted to the true formation by minimizing the error function. It is calculated as the square root of the sum of squares of differences between log responses in well and synthetic data computed as the output of the equation set solution (model parameters).

Depending on the software, the algorithms for solving the system of equations and the systems of equations themselves may differ. In most cases, also in Techlog (Schlumberger Co.), probabilistic models are used based on a matrix connecting the log responses with volumes of mineral contents and porosity. Additionally, all models include other parameters describing the formation as well as the measurement environment. Although the general principles used in commercial systems are similar, they differ in terms of the method of implementation and determination of uncertainty.

## SHORT PETROPHYSICAL CHARACTERISTICS OF CARBONATE AND SILICICLASTIC ROCKS

Carbonates are a mixture of limestone and dolomite rocks in various proportions (Folk 1980). They are mainly composed of calcite and dolomite minerals. Like other sedimentary rocks, most carbonates are built of grains. Part of the grains present in limestone are skeletal fragments of marine organisms. Other carbonate grains are ooids or onkoids, sometimes also calcite mud. The great variety of grain forms in carbonate reservoirs leads to various pore types, from the microscopic level to vuggy pores of several cm in diameter. After the sedimentation of particles, a diversity of physical and chemical processes starts to modify the rock structure, changing main characteristics as porosity and permeability in terms of compaction, diagenesis and others (Montaron 2005).

Porosity in carbonates can be grouped into three types: matrix porosity existing between grains, vug porosity due to the dissolution of calcite in water during diagenesis and fracture porosity caused by stress on the consolidated particles. A good petrophysical interpretation in these rocks depends on the application of more suitable models and the correct estimation of parameters.

Clean sandstones (without clay minerals) usually show high porosity and permeability (Folk 1980). They are frequently the goals in hydrocarbon and water prospection. Sandstones are built of clasts from different mineral material depending on depositional conditions. They are mainly composed of quartz, plagioclase, alkali feldspars, micas and various cements, like silica, clay, carbonate or irony. Sandstone clasts are of various size, shape, roundness and sorting. Porosity in sandstones is mainly primary and intergranular. Sandstones allow the filtration of water and other fluids and their effective porosity allows the storage of large volumes of hydrocarbons, as well as thermal or table waters. The petrophysical interpretation of clean sandstones is relatively easy and most theoretical and empirical equations are determined by scientists and engineers in reference to these formations. The presence of accessory minerals and clay ones lead to difficulties (Ballay et al. 2005).

### Role of clay minerals

The correct determination of shaliness is necessary in the quantitative interpretation of well logs in terms of the determination of porosity and hydrocarbon saturation. Shale volume has an impact on the determined parameters and may distort the interpretation process. Shale is an imprecise term which refers to fine-grained, clastic, sedimentary rock composed of a mixture of clay minerals and tiny fragments (pelite size) of other minerals like quartz, dolomite or calcite. Also, bound water volume in most of the models used is calculated together with shale volume. Various types of clay minerals and shale distributions in rock have different effects on well log records. From the well logging interpretation point of view, it is important to distinguish between four main minerals/groups of clay minerals: kaolinite, smectite, illite

and chlorite (Plewa & Plewa 1992, Schön 2011). The above-mentioned clay minerals have various elemental compositions, structures and textures, leading to differences in resistivity, ability to polarization, volume of bound water, density and others. The volume of selected clay minerals in rock formation can be approximated using appropriate cross-plots. Shale distribution in sandstones is variable and three different models of shale occurrence are defined as shown in Figure 1.



**Fig. 1.** *Models of shale distribution in sandstones (Schlumberger 1989, modified)*

In laminar forms of shaliness, clay minerals ($V_{sh}$) built the specific laminas with very low porosity ($\phi$), different from sandy laminas, thus total porosity of sandy-shaly formation is lowered because part of the rock volume is occupied by clays. Structural shale means the presence of clay minerals in the skeleton ($V_{sk}$), so porosity remains unchanged. In dispersed shaliness, clay minerals occupy part of the pore space, so porosity is distinctly reduced. Shale content causes reductions in effective porosity, permeability and decreases resistivity. Further clay presence complicates the proper determination of the volume and production of hydrocarbons.

In carbonates, clay volume is rather low but interpreters encounter its effects when estimating porosity and water saturation of limestone and dolomite reservoirs. The clay volume of the investigated Cuban reservoir formation was relatively low, and its presence was concentrated in the pore space. Schematic representation of different shale distributions in the Cuban carbonate reservoirs is presented in Figure 2. The high shale content observed in the Carpathian Foredeep formation was a mixture of the models presented in Figure 1 and it was not possible to differentiate the occurrence of forms on the basis of well logs.
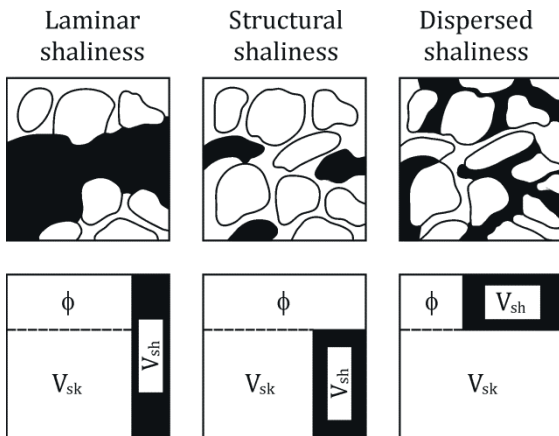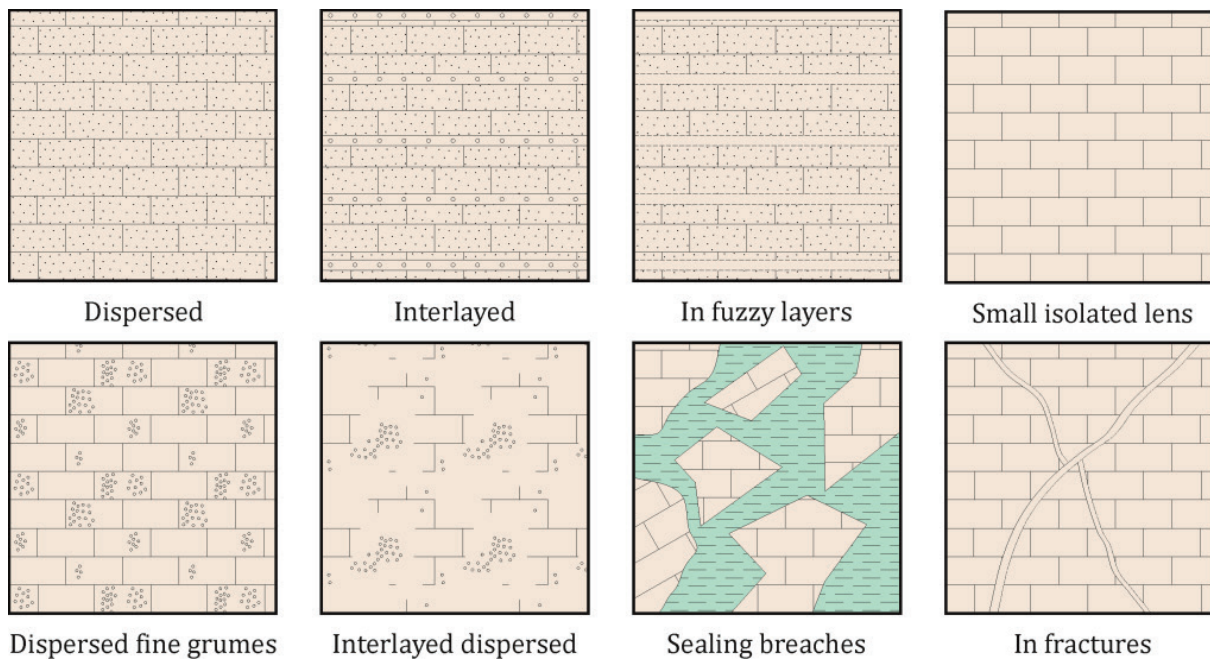


**Fig. 2.** *Schematic presentation of different forms of shaliness distribution in the Cuban carbonate reservoirs (Castro 1992)*

## PREPARING DATA

Well logging measurements made in a specific environment are influenced by various factors and require correction. Nowadays, corrections are usually made during data acquisition but before interpretation it is necessary to ensure good data quality. To fulfil this requirement, appropriate corrections were made (automatically or manually). Merging logs was done because measurements were made in different runs and the depths for equivalent position in the wellbore could be different. Run overlaps were investigated because they allowed the comparison of log results from the same point in the formation which were made in different wellbore parameters (resistivity and density of mud, well diameter etc.). Logs were edited to eliminate invalid data and a conversion to the same units was made. Core and log data were depth matched.

Measurements in the Cuban oilfield area were made using Schlumberger Co. tools, while in the Carpathian Foredeep gas deposit, Halliburton Co. tools were applied. An inventory of logs is presented in Table 1. Basic logs, i.e. resistivity, standard and spectral version of natural radioactivity measurement, bulk density, photoelectric absorption index and neutron porosity were measured in both cases, providing a platform for credible, comprehensive interpretation. In both cases, each of the five resistivity logs of different radii of investigation (RLA1, RLA2,... – high resolution laterolog array and HO01, HO03,... – high resolution array induction) were available and used in the qualitative interpretation to recognize porous and permeable formations. In the quantitative interpretation, resistivity logs of the smallest radius of investigation, RLA1 and HO01 were used for the water saturation ($S_w$) calculation in the flushed zone, while resistivity values from the log of the deepest radius of investigation, RLA5 and HO12, were used for $S_w$ determination in the virgin zone. In the carbonate rocks, the photoelectric absorption index played an important role as a factor enabling differentiation between carbonate components, because limestone and dolomite of high resistivity and low or very low natural radioactivity are not very diverse in bulk density, especially in the discussed case of the presence of organic matter. Spectral gamma ray, i.e. THOR and POTA curves in the A-1 well enabled the recognition of clay minerals. The transit interval time in the acoustic log, measured only in A-1 well in the Carpathian Foredeep gas deposit, provided additional information on gas saturation, important in the thinly-bedded, highly shaly Miocene reservoir.

*Table 1*
*Well logs used in the interpretation*

| Well | Depth interval [m] | Log | Mnemonic |
|---|---|---|---|
| **Cuban oilfield area** | | | |
| V-01X<br>V-02X | 3844–5823<br>4190–6004 | Caliper | CAL |
| | | Thermic | TEM |
| | | Electrical | RLA1, RLA2, RLA3, RLA4, RLA5 |
| | | Radioactive | SGR, CGR, NPHI, RHOB, PEF, THOR, URAN, POTA |
| **Carpathian Foredeep gas deposit** | | | |
| A-1 | 200–2230 | Caliper | CAL |
| | | Electrical | HO01, HO03, HO06, HO09, HO12 |
| | | Radioactive | GR, GRS, GG, NPHI, RHOB, PEF, THOR, URAN, POTA |
| | | Acoustic | DT |

## GEOLOGICAL SETTING

The lithology and stratigraphy of formations were briefly described in order to present the geological background and sedimentary conditions in which the studied reservoirs were recognized.

### Cuban oilfield area

The Cuban oilfield area is located in the Heavy Oil Northern Belt, in the eastern part of the Havana and Matanzas provinces, a place where more than 15 oilfields have been discovered. The discussed investigation only concerns West Varadero, located at N-NW of Hicacos peninsula as an enlarged structure in the form of a belt that continues from the town of Camarioca to Varadero. From all of the wells drilled in this part of the oilfield, only one (presented in the paper as V-02X) drilled Upper Paleocene-Lower Eocene clay sediments after the Upper Jurassic (Fig. 3A). Traps in this area are of the structural type, with folds and thrusting faults (Fig. 3B). This is the Cuban Thrust-Belt and is built of several thrusting mantles or sheets, belonging to the same tectonostratigraphic unit (Placetas) (López et al. 2012, López et al. 2015). The same situation, but on a more general scale, is observed in Figure 3B (Moretti et al 2003). It is distinctly visible here how units 2, 3 and 4

(Cretaceous and Jurassic) sometimes lie upon unit 1 (Tertiary-Paleocene, Eocene). The picture presented in Figure 3A results from the specific geological structure (thrusting) and the trajectory of the well, because the potential hydrocarbon accumulations are in the thrust mantles or sheets. A simplified structure is presented after analyzing geological cross sections, seismic and well logging results. Litho-stratigraphy of the presented units is included in Table 2.

According to the investigations, which were based on 3D seismic data and the existing well logging results of the Cuban Oil Investigation Centre (CEINPET) in 2012, it was concluded that the region is made up of several grand units or formations, that feature throughout the whole of the Cuban Thrust-Belt (López et al. 2012). Rocks forming these units are considered to be the following ones: 1) post-orogenic, 2) syn-orogenic Lower Eocene, 3) ophiolites (Cretaceous Volcanic Arc), 4) syn-orogenic Lower Cretaceous, 5) Medium Cretaceous continental margin carbonates, 6) Upper Paleocene-Lower Eocene syn-orogenic rocks, 7) Upper Jurassic-Neocomian (Lower Cretaceous) continental margin carbonates (Fig. 3A, Tab. 2). The last unit (Upper Jurassic-Oxfordian) is formed of syn-rift clastic rocks (claystones, sandstones, very heterogenous limestones).
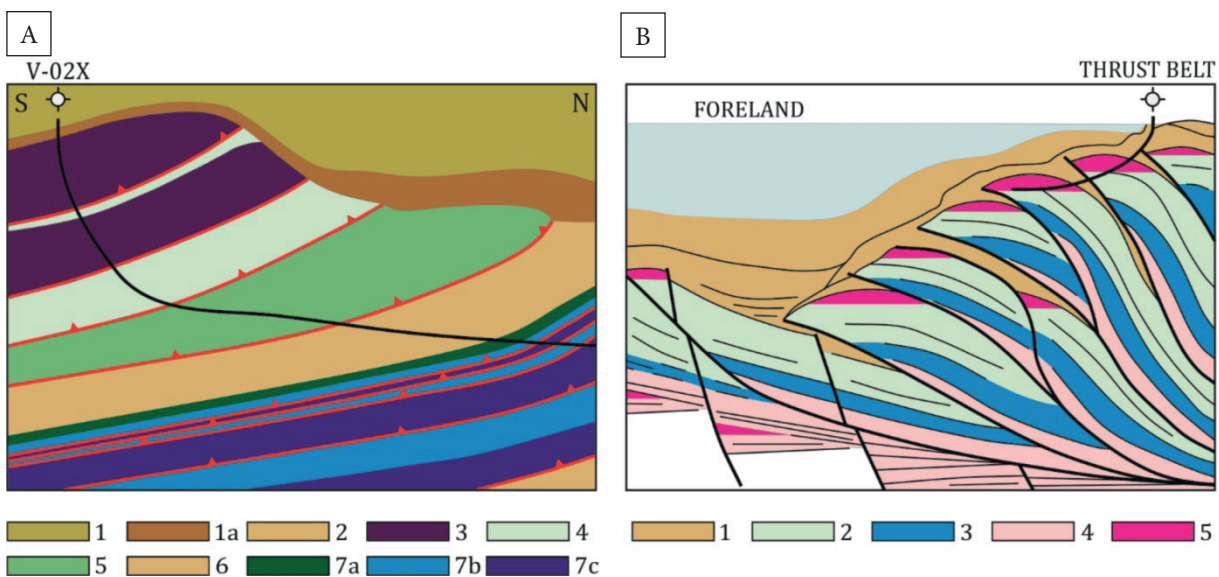


***Fig. 3.*** *Simplified structure of the Cuban Oilfield area (López et al. 2015, modified) (A); explanations are included in Table 2; synthesis of the play concept of the northwest off shore Cuba petroleum system (B): 1 – Tertiary, 2 – Cretaceous, 3 – Jurassic – mainly carbonates, 4 – Jurassic – mainly clastics, 5 – potential accumulation (Moretti et al. 2003, modified)*

*Table 2*
*Litho-stratigraphy of formations presented in Figure 3A*

| Formation | Stratigraphy | Lithology |
|---|---|---|
| 1 and 1a | Postorogenic | Phosilypheros limestones, dolomites, marls |
| 2 | Syn-orogenic Lower Eocene | Argillites and some carbonate fragments |
| 3 | Ophiolites (Cretaceous Volcanic Arc) | Serpentinite mélanges and ophiolites |
| 4 | Syn-orogenic Lower Cretaceous | Compact carbonates (hard limestones) |
| 5 | Medium Cretaceous | Continental margin carbonates |
| 6 | Syn-orogenic Upper Paleocene-Lower Eocene | Claystone, mainly argillite |
| 7a | Upper Jurassic-Neocomian (Lower Cretaceous) | Continental margin carbonates |
| 7b | Upper Jurassic, Tithonian | Carbonates, naturally fractured and lixiviated |
| 7c | Upper Jurassic Kimmeridgian | Carbonates, naturally fractured and lixiviated |

Units 6 and 7 are found in the profiles of wells studied in this research. The presented oilfield constitution responded to a typical geology of duplex structures or scales that repeat themselves through faults and horsts. Upper Jurassic reservoirs are carbonates, naturally fractured and lixiviated.

Seal rocks consist of Paleogene clays placed as an unconformity above the grand units. A geological section over the V-02X well made from the seismic data shows all of the sheets that repeat themselves from south to north, starting with ophiolites, Upper Cretaceous syn-orogenic formation, Medium Cretaceous sheets also separated by Upper Cretaceous clays, until reaching the Upper Jurassic-Neocomian (Lower Cretaceous) sheets that continue repeating through the horsts and faults, without the presence of Upper Paleocene-Lower Eocene clays between the sheets (López et al. 2015).

**Carpathian Foredeep gas deposit**

Siliciclastic Miocene formations are presented on the basis of an exemplary geological profile of well A-1. The borehole, located in the middle part of the Carpathian Foredeep, drilled the Miocene, Jurassic, Triassic, Carboniferous and Precambrian formations to a depth interval of 200–2551 m (Syrek-Moryc 2006, Filo 2006–2007). The Miocene sandy-shaly, thin-bedded formations and Carpathians flysch marginal zone reservoirs were the goals of hydrocarbon prospection for decades in Eastern-Southern Poland (Karnkowski 1999). Exploration works were focused on the Miocene, Early Cretaceous and Jurassic formations.

In the discussed case, prospecting attention was directed on the autochthonous Miocene formations (200–2028 m), built of the Sarmatian and Badenian beds. The full profile of the autochthonous Miocene consisted of the Sarmatian and Upper Badenian thinly bedded sand-, mud- and claystones, Middle Badenian anhydrites intercalated with shale layers and Lower Badenian mudstones and marly mudstones. Mesozoic sediments represented by the Jurassic deposits (202 m of thickness) are composed of Malm limestones and dolomites and Dogger sandstone-mudstone deposits. In the primary (cross-plots) and comprehensive interpretation, the Dogger deposits are not included.

**TECHLOG PROCEDURES USED IN THE INTERPRETATION**

In both cases, the interpretation was made using Techlog (Schlumberger Co.) software. Procedures of the Quanti module were adopted for the Cuban oilfield data of the V-01X and V-02X wells, Quanti Elan module was applied for the Miocene gas field data interpretation of the A-1 well.

**Qualitative interpretation**

Before conducting the quantitative interpretation, parameters were determined that might improve

results. The primary mineral composition of the rock matrix model was built on the basis of the geological macroscopic description of cores and cuttings obtained during the drilling process. In addition, the cross plots turned out to be very useful for rough lithology identification. In both cases, bulk density (RHOB) vs. neutron porosity (NPHI) cross plots were constructed (Fig. 4A, B). They allowed for the preselection of the dominant lithology types. Comparison of the plots showed a more distinct differentiation in the Cuban carbonate units (Fig. 4A). Within the Carpathian Foredeep log data (Fig. 4B), the Miocene siliciclastic rocks dominated but the division between them and the Jurassic sediments was not very precise, despite the lithology overlay. Another log data crossplot of bulk density (RHOB) vs. transit interval time (DT) helped with the determination of the mineral composition (Fig. 5). The position of the data between lithology lines and marked points of

specific minerals were helpful in the selection of rock types.

Cross-plots of Figure 4 were generated assuming mud filtrate density equal to 1 g/cm³ in the Cuban data case and 1.16 g/cm³ in the Carpathian Foredeep data. Visible differences in the overlays shape of Figure 4A, B resulted from the data being recorded by different logging devices and density of mud filtrate. In Figure 4A, the litho-stratigraphy zonation is presented using colours and all the units in the discussed reservoir zone can be observed: unit A depicts a geological formation from the Upper Cretaceous, B, C, E, F, G, H, I and J illustrate formations of the Upper Jurassic and D representing synrift clastic (shaly) rocks. In the discussed case, in the majority of data, a shift over the limestone line is the result of the mentioned clastic lithology. The reservoir was mainly built of carbonates with some clay content. Unit D is the exception because it is a very heterogeneous formation with high clay content.
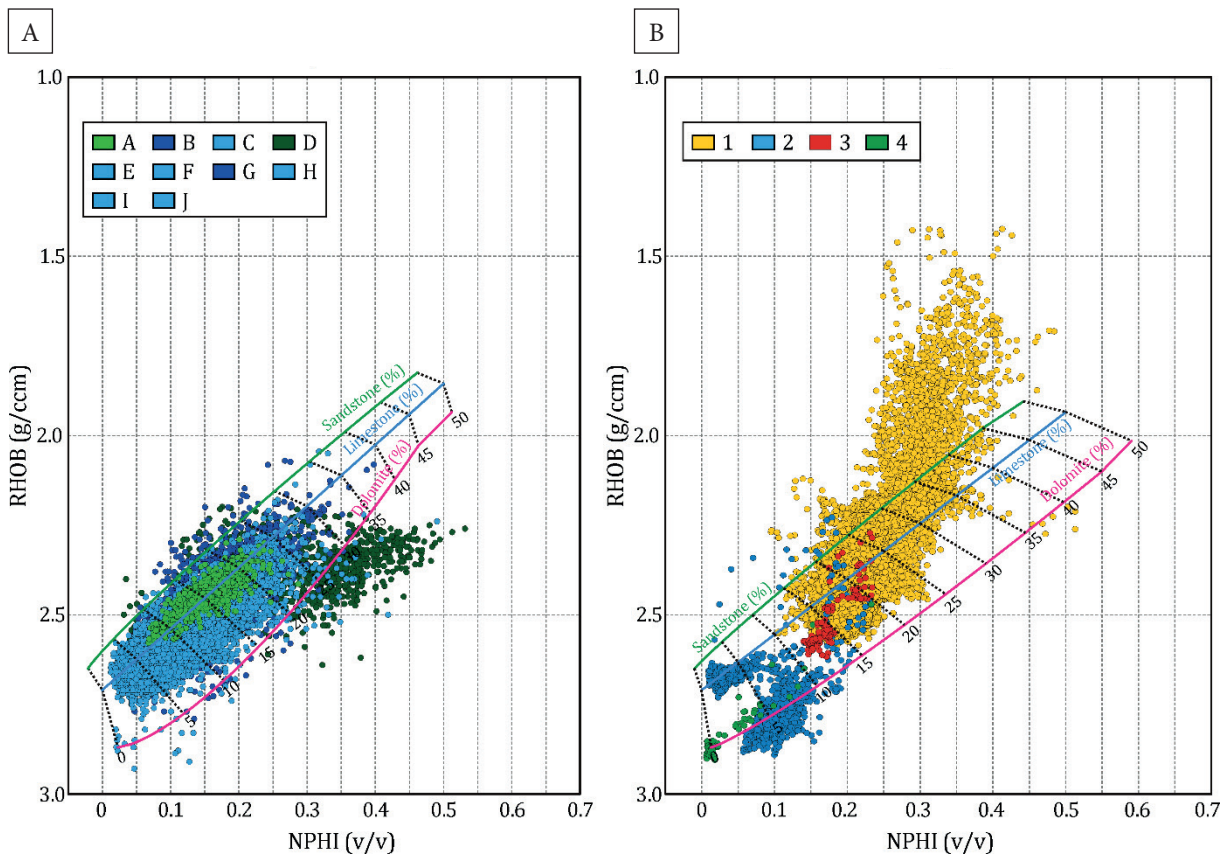


***Fig. 4.*** *RHOB vs. NPHI cross-plot: A) Cuban carbonate formation; A–J – formations/units according to Figures 3 and explanations in the text; B) Carpathian Foredeep siliciclastic formation: 1 – Miocene, Sarmatian and Upper Badenian shaly sandstones, 2 – Jurassic, Malm carbonates, 3 – Middle Badenian anhydrites, 4 – Lower Badenian mudstones and marly mudstones*

The shift of the Miocene, Sarmatian and Upper Badenian sandstone data in the Carpathian Foredeep to the higher NPHI values resulted from the high shaliness of the formation (Fig. 4B). The position of the group of Sarmatian and Upper Badenian (yellow) data over the sandstone line in Figure 4B can be explained by gas saturation. Middle Badenian anhydrites are visible with high bulk density and very low neutron porosity in the left lower corner of the cross-plot (Fig. 4B). Lower Badenian mudstones and marly mudstones fit well into shaly-sandy samples without any gas saturation (Figs. 4B, 5). A small group of the Sarmatian and Upper Badenian data located over the upper line presented in the RHOB vs. DT cross-plot (Fig. 5) also confirmed low gas saturation obtained in the next interpretation step. Illite and micas shown as dominated clay minerals that is in Figure 6 also explain the lowering of bulk density. The presented cross-plots (Figs. 4, 5) confirmed carbonate formation in the Cuban oil field and revealed a heterogeneous Miocene formation composed of quartz, high volume of clay minerals and carbonate cements proved in laboratory results (Filo 2006–2007). The approximate total porosity ranged from 5 to even 30% in the carbonates and showed even 45% in the Miocene sandstones.
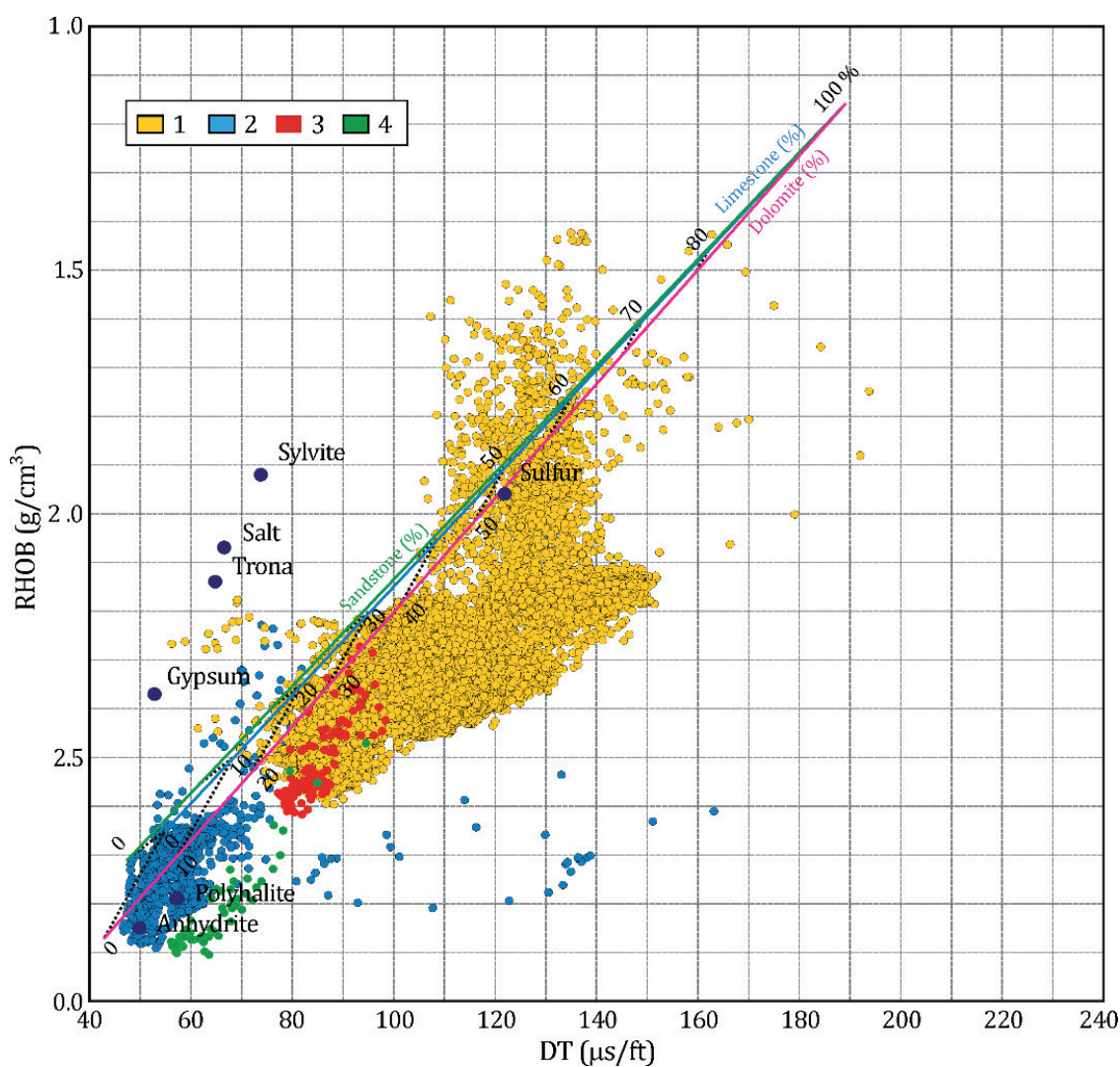


**Fig. 5.** *RHOB vs. DT cross-plot for the Carpathian Foredeep formations with lithology identification overlay: 1 – Miocene, Sarmatian and Upper Badenian shaly sandstones, 2 – Jurassic, Malm carbonates, 3 – Middle Badenian anhydrites, 4 – Lower Badenian mudstones and marly mudstones*
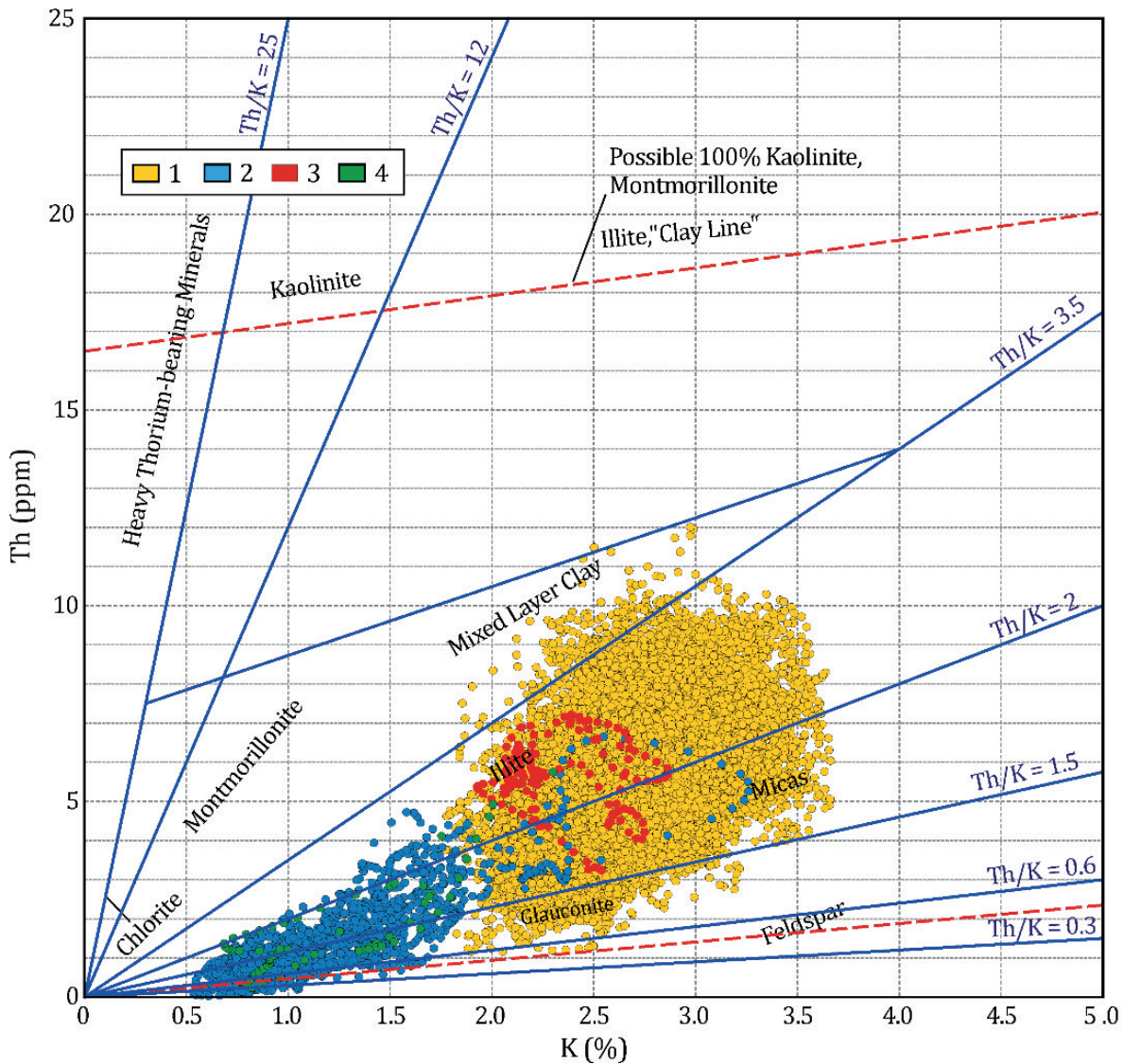
**Fig. 6.** *Clay mineral identification cross-plot, Carpathian Foredeep sample, A-1 well: 1 – Miocene, Sarmatian and Upper Badenian shaly sandstones, 2 – Jurassic, Malm carbonates, 3 – Middle Badenian anhydrites, 4 – Lower Badenian mudstones and marly mudstones*

## Quantitative interpretation

Techlog software allowed the quantitative interpretation to be made in two different ways. Using the Quanti module, the calculation of shale volume, porosity and saturation was made step by step. Quanti Elan module provided the stochastic solution based on probabilistic, multicomponent model proposed by interpreter. All petrophysical parameters were the outcomes of the comprehensive interpretation. Generally, the interpretation of the carbonate formation was done using Quanti module procedures, while the solution in the sandy-shaly Miocene formation was obtained using Quanti Elan module. Interpretation in the carbonate formation was also the guide showing how the procedures in the Quanti module work, while Quanti Elan revealed abilities and difficulties in the siliciclastic rocks interpretation. The sequence of shaliness, porosity, saturation and lithology determination is described and illustrated by means of the Cuban data samples. The Quanti Elan interpretation was applied for the Carpathian Foredeep Miocene formations.

## *Shale or clay volume*

Information about shaliness in a formation is crucial for selecting the proper parameters for the interpretation. Clay minerals impact on the matrix composition and reservoir parameters depends on their morphology, structure and texture, cation exchange capacity and elemental composition (Akhir et al. 2015). Shale volume estimation was made on the basis of natural gamma radioactivity curve (GR). In both cases, the computed gamma ray curves (from the spectral gamma log SGR) were used in order to not take the presence of uranium into account. This was because the uranium volume curve was treated as an indicator of the presence of organic matter (also, fractures with collected uranium compounds), while the other two components of the natural gamma radiation, potassium and thorium volume curves (POTA, THOR) were perceived as the main indicators of clay radioactivity.

The linear model is best suited for the Cuban carbonate formations:

$$V_{sh} = \frac{CGRlog - CGRmin}{CGRmax - CGRmin} \left[ v/v \right] \tag{2}$$

where:

$V_{sh}$ – shale or clay volume [v/v],

CGRlog – current values of the computed GRlog (API),

CGRmin – minimum value selected from the curve of the computed GRlog, it represented a rock with no clay content (API),

CGRmax – maximum value selected from the computed GRlog, it represented a clay rock or a rock with high clay content (API).

Dominating clay minerals were determined using cross-plot of thorium vs. potassium (Klaja & Dudek 2016). The Miocene sandy-shaly formation sample is presented in Figure 6. The example showed that the Miocene formation is mostly composed of illite and micas.

## *Porosity*

Total porosity for the Cuban data was directly obtained from the neutron log because the measuring tool was calibrated in porosity units. On the other hand, the recorded density values, RHOB were transformed into total porosity using the Quanti module equation:

$$\phi_d = \frac{\rho_{ma} - RHOB}{\rho_{ma} - \rho_f} \tag{3}$$

where:

$\phi_d$ – porosity estimated from the density log [v/v],

$\rho_{ma}$ – rock matrix density [g/cm³],

RHOB – bulk density from density log [g/cm³],

$\rho_f$ – density of fluid in pores (mud filtrate) [g/cm³].

Total porosity ($\phi_t$) was assumed as the average between $\phi_d$ and the values of neutron log of porosity ($\phi_n$).

Effective porosity was obtained by the subtraction of shaliness, i.e. clay occupying the pore space from the total porosity:

$$\phi_e = \phi_t - V_{sh} \cdot \phi_{sh} \tag{4}$$

where:

$\phi_e$ – effective porosity [v/v],

$\phi_t$ – total porosity [v/v],

$V_{sh}$ – shale or clay volume [v/v],

$\phi_{sh}$ – porosity of shale [v/v].

Other formulas are proposed in the Quanti module for total and effective porosity calculations using other logs. In the presented Cuban data, the neutron and density logs were only used because of the non-existence of sonic logs. In the interpreted geological profiles, the number of available cores was limited, so there were no reliable laboratory results to make the confirmation.

## *Fluid saturation*

Due to the nature of electrical current flow in rocks, the majority of saturation models applied in reservoir interpretation use resistivity logs. In any equation, water/ hydrocarbon saturation is a function of resistivity of the formation and there are a series of parameters that need to be properly evaluated: formation temperature, water formation resistivity, mud filtrate resistivity, tortuosity coefficient, cementation and saturation exponents. Computer systems propose some default values that work in most cases, but precise values should be obtained by means of laboratory

measurements. The proper formation water resistivity and the cementation exponent was found on the basis of Pickett plot (Aguliera 1995, Asquith & Krygowski 2004). This methodology is based on the Archie equation for a clean formation (Archie 1942). In a simple way, in the cross-plot of $\phi_t$ (total porosity) vs. $R_t$ (formation resistivity) in two logarithmic scales the line that fits the lower resistivity edge of cloud of data points represents the 100% water saturation and the intercept with the line of 100% porosity, represents the formation water resistivity. Cementation exponent ($m$) was determined from the slope of the above-mentioned line. A theoretical plot illustrating Pickett methodology utilization is presented in Figure 7. Analytically, Equation (5) describes the process of $m$ exponent determination:

$$\mathrm{Log}(R_t) = -m\,\mathrm{Log}(\phi_t) + \mathrm{Log}(a\cdot R_w) + \\ + \mathrm{Log}(R_t / R_o) \quad (5)$$

where:

$R_t$ – formation resistivity [Ω·m] when partially water, partially hydrocarbon saturated,

$R_o$ – formation resistivity [Ω·m] when fully water saturated,

$R_w$ – formation water resistivity [Ω·m],

$m$ – cementation factor [–],

$\phi_t$ – total porosity [v/v],

$a$ – tortuosity coefficient [–], usually equal to 1.

Cementation factor m values resulting in the Cuban reservoir interpretation in wells V-01X and V-02X are presented in Table 3. The obtained values are lower in comparison to the Archie solution ($m = 2$ is recommended for clean carbonates). This is related to the level of fracturing in these rocks. Once $R_w$, temperature and m were known, it was accordingly checked that they matched known water salinity. This was known in the Cuban area due to previous studies: 40,000–60,000 ppm. The mud filtrate resistivity and its temperature were taken from the well reports.

*Table 3*

*Temperature, formation water resistivity and cementation exponent for wells in study*

| Well | Average temperature [°C] | Resistivity of formation water [Ω·m] | Cementation factor [m] |
|------|-------------------------|--------------------------------------|------------------------|
| V-01X | 55.0 | 0.100 | 1.6 |
| V-02X | 50.0 | 0.085 | 1.5 |
| A-1 | 50.2 | 0.07 | 1.7 |

Pickett plot was also prepared for the Carpathian Foredeep data (Fig. 8) to determine the cementation factor $m$ and formation water resistivity $R_w$ these were important for the correct water/gas saturation calculation. The high shale content of formations and the mix of clay minerals resulted in a low value of $m = 1.7$ (Tab. 3).
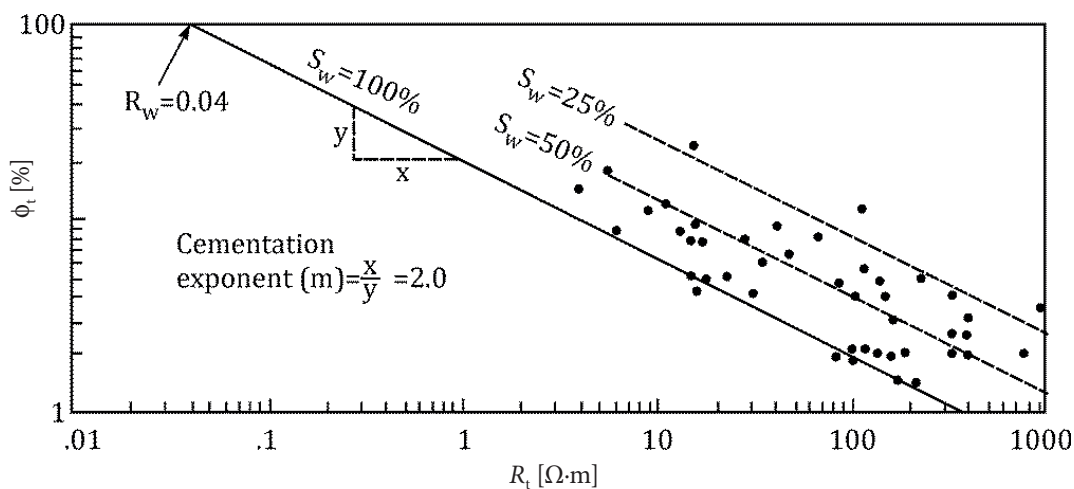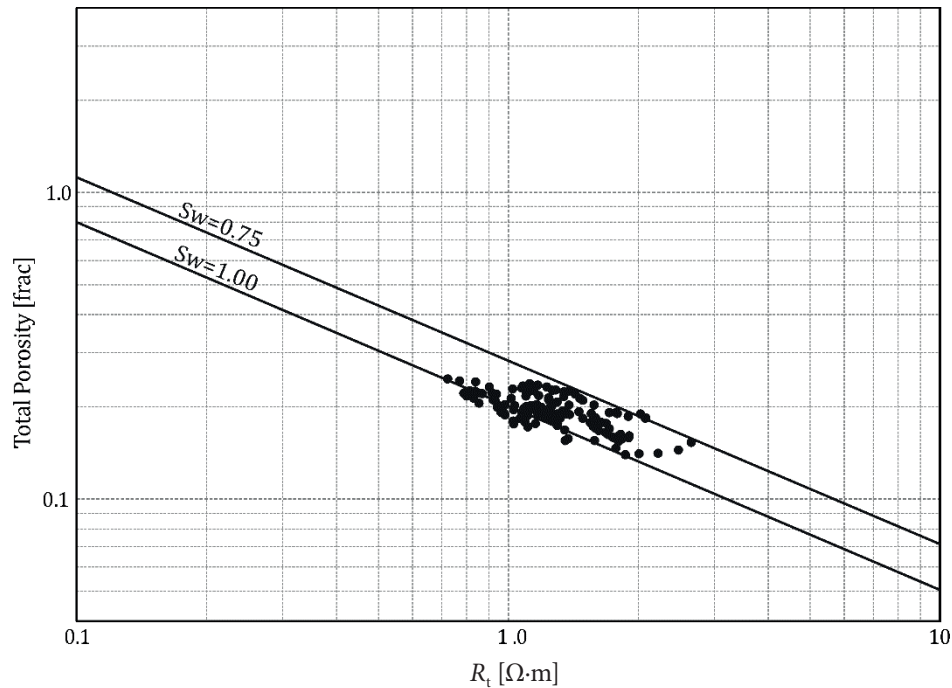


*Fig. 7. Pickett methodology utilization*

**Fig. 8.** *Pickett plot for the Carpathian Foredeep data*

## Saturation models

In the presented carbonate and siliciclastic rocks, the best results for water/hydrocarbon saturation were estimated using the Archie equation for the Cuban profiles, assuming their almost clean formations (6) (Archie 1942), and a modified Simandoux formula for Carpathian profile as for shaly deposits (7) (Crain 2002). Within the Archie model, it was simply assumed that water saturation $S_w$ was a function of formation resistivity $R_t$ and water formation resistivity $R_w$, while modified Simandoux model included the clay resistivity impact:

$$S_w^n = \frac{a}{\phi^m} \cdot \frac{R_w}{R_t} \qquad (6)$$

(for symbols see above).

$$S_w = \frac{-\dfrac{V_{cl}}{R_{cl}} + \sqrt{\left(\dfrac{V_{cl}}{R_{cl}}\right)^2 + \dfrac{4}{R_t} \cdot \dfrac{\phi^m}{a \cdot R_w \cdot (1 - V_{cl})}}}{2 \cdot \dfrac{\phi^m}{a \cdot R_w \cdot (1 - V_{cl})}} \qquad (7)$$

where:

$R_{cl}$ – clay resistivity [Ω·m],
$V_{cl}$ – clay volume.

### Effective intervals

In general, the production properties of a reservoir rock are a function of its ability and capacity to store hydrocarbons. The saturation ability/ storage capacity and the permeablity/ fluid flow of the pore space is crucial. Also, shaliness plays and the type of fluids filling the pore space play an important role in determining reservoir/ production properties.

In order to find the effective intervals, it was necessary to determine the cut off values of clay volume, effective porosity and water saturation. The Cumulative Hydrocarbon Column technique (Computing Petrophysical cut off 2015) was used at one well (V-01X). The presented elbow points were very important because they defined the cut off values to store hydrocarbons. With increasing shaliness, the possibility of storing and transporting hydrocarbons is not possible.

The concept of the hydrocarbon column (HCOL) calculation in a formation was based on the equation:

$$HCOL = \phi_e \cdot (1 - S_w) \cdot \Delta H \qquad (8)$$

where:
HCOL – hydrocarbon column [m],
$\Delta H$ – height interval [m].

Total hydrocarbon column, THCOL [%], was defined according to the formula (9):

$$THCOL = HCOL/HCOLA \qquad (9)$$

where HCOLA – hydrocarbon column for the whole interval [m].

It was the equivalent height of the pure hydrocarbon column contained in a zone of thickness $\Delta H >$ HCOL.

To calculate the cut off value for $V_{cl}$, the top and base of the interest zone were defined, THCOL was computed for all the values without restrictions. Then a regular decreasing of values for $V_{cl}$ cut off was applied, that is $V_{cl}$ cut off = (100%, 95%, 90%, ..., 0%) and THCOL was computed, rejecting rocks for which $V_{cl} > V_{cl}$ cut off. Using this, a set of points of $V_{cl}$ cut off and THCOL was obtained, these points were plotted (Fig. 9A), and the elbow point (i.e. the point where the total HCOL started to not having variations) was the ultimate cut off value for the $V_{cl}$.

Cutoff value for the effective porosity, PHIE, was calculated in the same way as the porosity values, where $V_{cl} \leq V_{cl}$ cut off and PHIE $\geq$ PHIE cut off, making variation of the effective porosity from 0.4 to 0 regarding to the total HCOL (Fig. 9B).

Water saturation $S_w$ cut off value was determined, keeping cut off values of $V_{cl}$ and PHIE fixed and making variations of $S_w$ from 1 to 0 regarding total HCOL (therefore $V_{cl} \leq V_{cl}$ cut off, PHIE $\geq$ PHIE cut off and $S_w \leq S_w$ cut off). Finally, again the elbow point was taken as the water saturation cut off value (Fig. 9C).

After this analysis of the well V-01X of the Cuban oilfield, the cut off values were assumed as $V_{cl}$ = 25%, PHIE = 6% and $S_w$ = 40%.

### Lithology model

In the case of the Cuban oilfield, a lithology model was estimated using the Lithology Computation tool of the Quanti module. This is designed to calculate up to four lithologies based on the following input parameters: consistent to above effective porosity, shale volume, water saturation and bulk density. The relative proportions of the different lithologies were based on the lithology cross-plots $DT_{ma}$ vs. $RHOB_{ma}$ and $U_{ma}$ vs. $RHOB_{ma}$. First the apparent matrix properties $RHOB_{ma}$, $DT_{ma}$, Uma were calculated. With the minimum input parameters only, two lithologies were calculated based on $RHOB_{ma}$ only, with an additional input (DT or PEF/U) a third lithology can be estimated while it is possible to calculate a fourth one by using both. In the presented case, shale volume, water saturation, bulk density and photoelectric absorption index with its volumetric cross section ($U$) were used as inputs because of the lack of a transit interval time.

The following matrix parameters were used:
- sandstone: PEF = 1.8 barn/electron; U = 4.8 barn/cm³; RHOB = 2.65 g/cm³;
- limestone: PEF = 5.1 barn/electron; U = 13.8 barn/cm³; RHOB = 2.71 g/cm³;
- dolostone: PEF = 3.1 barn/electron; U = 9 barn/cm³; RHOB = 2.85 g/cm³.

Finally, the lithology model was built of: dolomite ($V_{Dol}$), limestone ($V_{lime}$) and sandstone ($V_{sand}$).
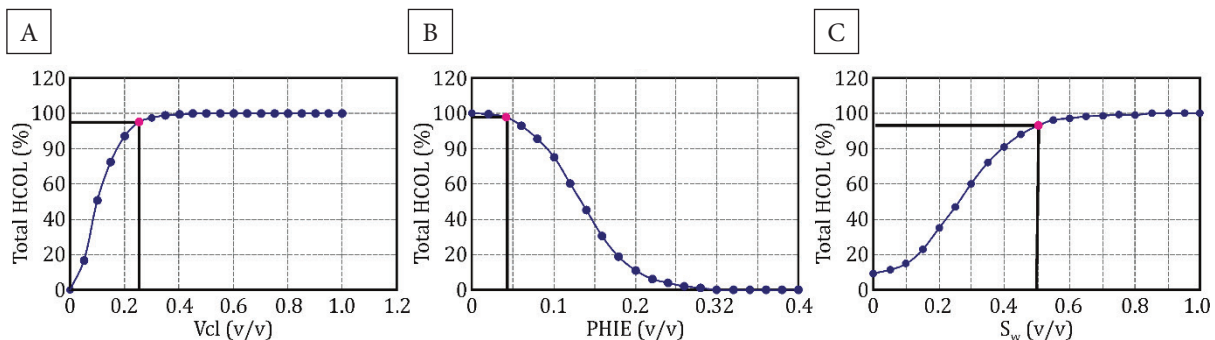


**Fig. 9.** *Results of the selection of the cut off value in well V-01X: A) clay volume cut off; B) effective porosity cut off; C) water saturation cut off*

### Quanti Elan

Comprehensive interpretation of the well A-1 well logs at the Carpathian Foredeep was done using the Quanti Elan module. This is a statistic model method based on a probabilistic and multicomponent approach. (Fig. 10).

In the presented matrix A, B, C, D, E, F and G mean unknowns, i.e. mineral component volumes and pore fluids volumes. 1, 2, 3, 4, 5, 6, 7 are log responses from rock formation measurements, $\alpha_{a,1}$ are matrix parameters typical for each mineral and also parameters of pore fluid.

Models declared by sets of equations (Fig. 10) were defined several times in the interpretation zone of 1000–2000 m. The number of model components was equal or smaller than the available

logs. The selection of minerals of the model was made on the basis of a qualitative interpretation, core samples and cuttings analyses and information from mud logging. The best model adoption was done using the trial and error method. Quartz, feldspar, calcite, dolomite and shale as a group of clay minerals were considered as suitable mineral components for the Carpathian Foredeep sandy-shaly rocks. Some tests with various mineral composition were done. The best solution was based on quartz, calcite and shale, built of illite. The formation was saturated with formation water, the parameters of which were determined using a Pickett plot (Tab. 3). Based on the analysis of nearby wells, gas was chosen as a possibly occurring hydrocarbon.

$$
\begin{bmatrix}
\alpha_{a,1} & \alpha_{b,1} & \alpha_{c,1} & \alpha_{d,1} & \alpha_{e,1} & \alpha_{f,1} \\
\alpha_{a,2} & \alpha_{b,2} & \alpha_{c,2} & \alpha_{d,2} & \alpha_{e,2} & \alpha_{f,2} \\
\alpha_{a,3} & \alpha_{b,3} & \alpha_{c,3} & \alpha_{d,3} & \alpha_{e,3} & \alpha_{f,3} \\
\alpha_{a,4} & \alpha_{b,4} & \alpha_{c,4} & \alpha_{d,4} & \alpha_{e,4} & \alpha_{f,4} \\
\alpha_{a,5} & \alpha_{b,5} & \alpha_{c,5} & \alpha_{d,5} & \alpha_{e,5} & \alpha_{f,5} \\
\alpha_{a,6} & \alpha_{b,6} & \alpha_{c,6} & \alpha_{d,6} & \alpha_{e,6} & \alpha_{f,6} \\
\alpha_{a,7} & \alpha_{b,7} & \alpha_{c,7} & \alpha_{d,7} & \alpha_{e,7} & \alpha_{f,7}
\end{bmatrix}
\begin{bmatrix}
A \\ B \\ C \\ D \\ E \\ F \\ G
\end{bmatrix}
\begin{bmatrix}
1 \\ 2 \\ 3 \\ 4 \\ 5 \\ 6 \\ 7
\end{bmatrix}
$$

$$1 = A + B + C + D + E + F + G$$

**Fig. 10.** *Matrix of equation system using in Techlog Software (Techlog Online Help 2015, modified)*

## RESULTS

Results of the interpretation made using Quanti module (Techlog) in V-02X well in the Cuban oilfield are presented in Figure 11. Track configurations are described as follows: the first track contains caliper, second – zonation symbols, third – CGR (computed gamma ray), SGR (standard gamma ray), PEF (photoelectric absorption index), fourth – resistivity curves of high resolution laterolog array tool (HRLA), with a different investigation radius, fifth – RHOB (bulk density) and NPHI (neutron porosity) curves, sixth – uranium, URAN, thorium, THOR and potassium, POTA contents, seventh – track

contains the lithology model, eighth – total, PHIT and effective, PHIE porosities, ninth – track shows water saturation $S_w$ and the last one contains the pay zones or effective intervals (presented in red color). Clay volume is pretty low in all of the reservoir zones (units), rarely exceeding 25%, except of zone D which is built as a shale layer. All reservoir zones (units) identified in Figure 11 (marked with blue and green colors) are also visible in Figure 4A. Total and effective porosity values are relatively high for carbonates, total porosity ranges from between 3–23%, with the average value equal to 15%, while effective porosity ranges from between 1–20%, with the average equaling 10%.
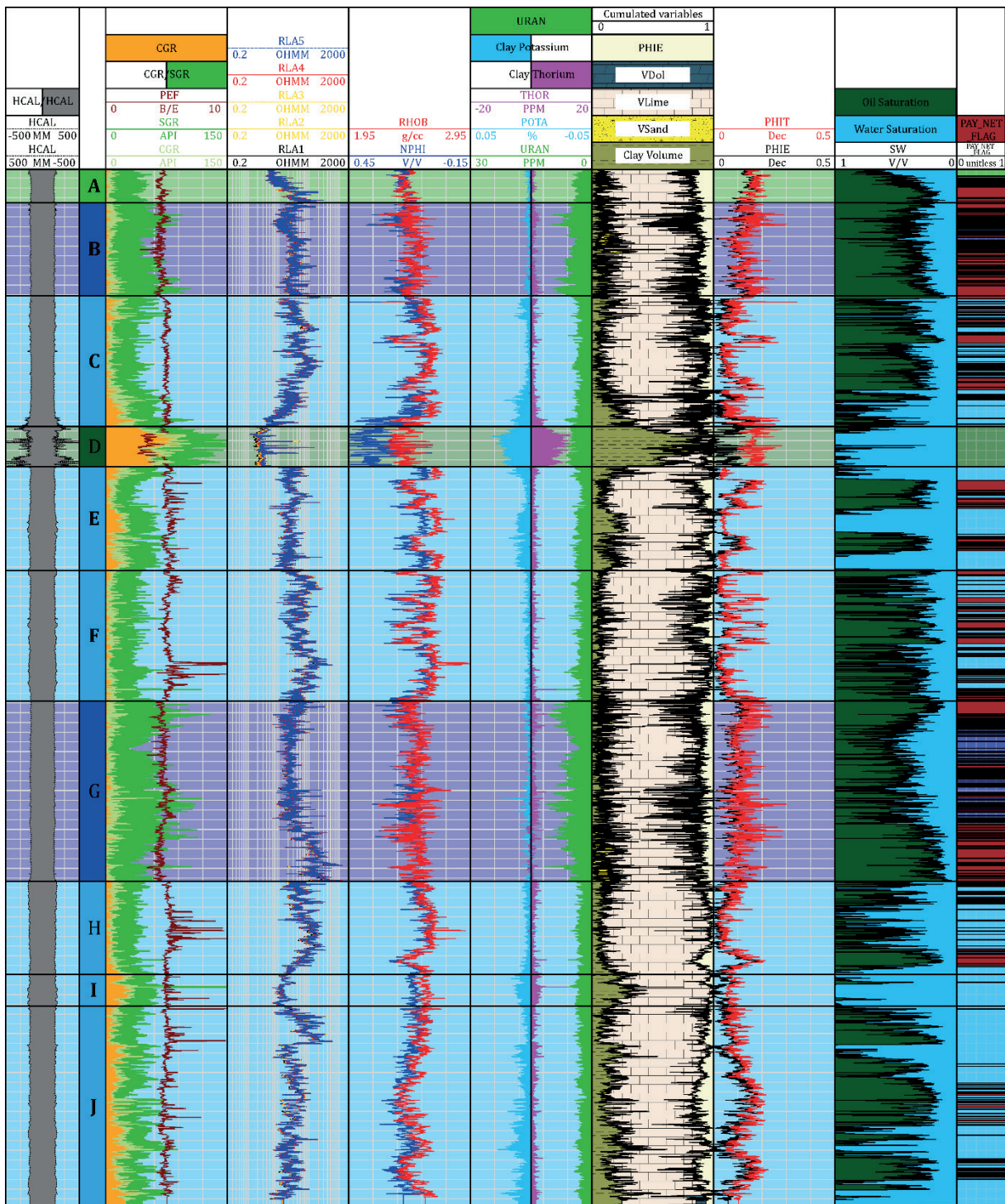
**Fig. 11.** *Interpretation plot of the V-02X well, vertical scale 1:5000 (tracks description presented in the text)*
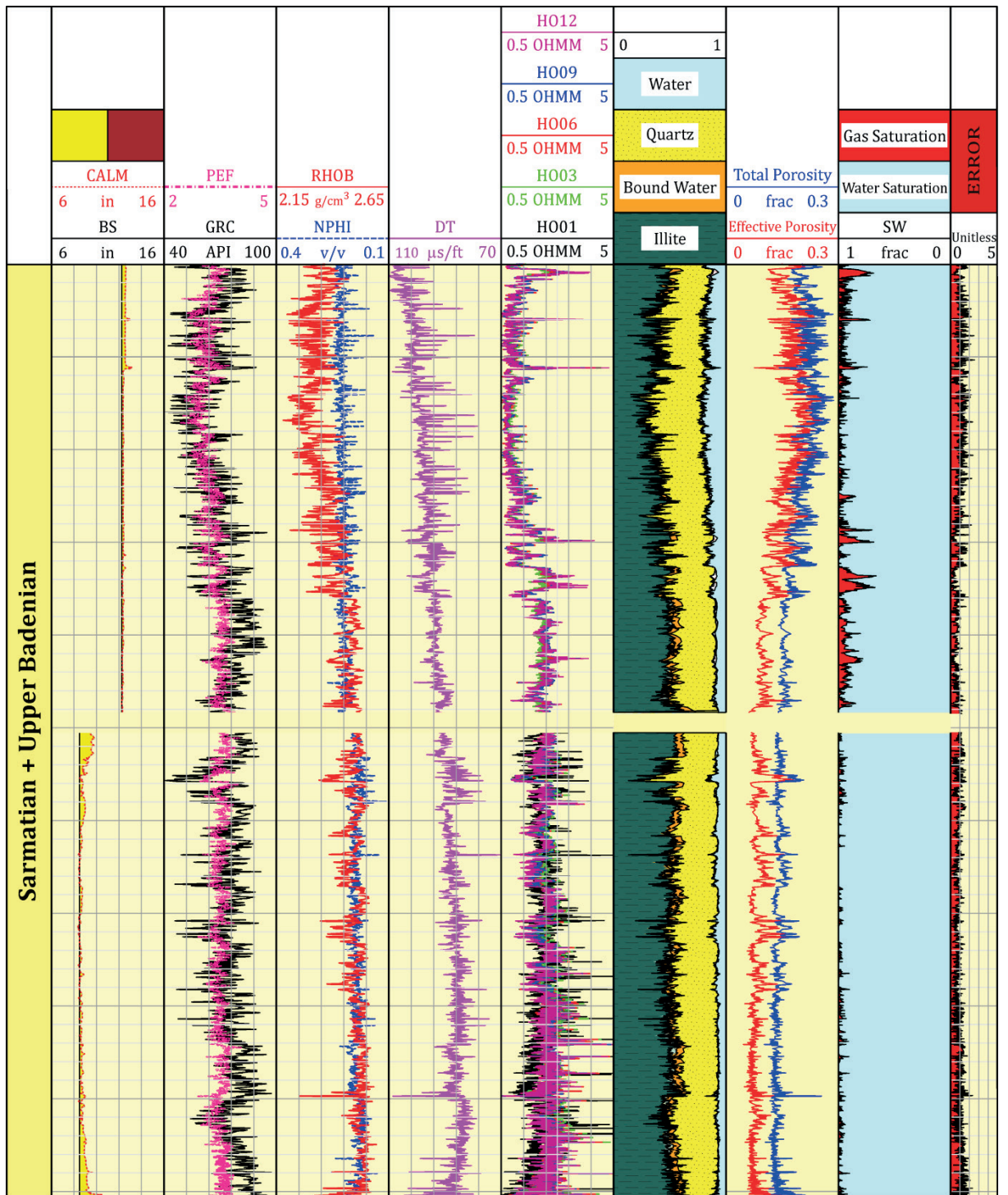
**Fig. 12.** *Results of the interpretation in the A-1 well, vertical scale 1:5000 (tracks description presented in the text)*

The last track presents saturation, colored in blue for water and in green for oil. In the reservoir water, saturation almost never exceeds 40%, in general being around 30%, and showing good potential for oil production in the area.

Figure 12 shows the results of the comprehensive interpretation of well logs in the Miocene formation in well A-1 at the Carpathian Foredeep. The track description is quite similar to Figure 11. DT in the fifth track means show the acoustic log transit interval time and HRAI in the sixth track show resistivity curves from high resolution array induction tool. Clay volume is even higher than 50%, in some intervals and is represented by illite. Shaliness causes a distinct decrease in effective porosity, PHIE, which is relative to total porosity, PHIT, and leads to low value of movable fluids. The volume of calcite was interpreted by the algorithm as insignificant (just invisible in the plot). Gas saturation presented in the last track is very low and occurs only in the upper part of interval. There is no potential for hydrocarbon production in this area.

## SIMILARITIES AND DIFFERENCES

Techlog turned to be very useful software for the interpretation of carbonate and siliciclastic reservoirs, despite their differences in geological structure and the sedimentological environment of the rocks. Litho-porosity and saturation interpretation in the Mesozoic carbonates and sandy-shaly Miocene formations was done on the basis of similar sets of logs. The difference was related to resistivity logs – an array laterolog in carbonates case and array induction logs in shaly formations. This was in accordance with the physical basis and a pattern of current flow of both types of measurements. First, the laterologs were most suitable as resistivity logs for high resistivity formations and relatively low water-based mud resistivity. Secondly, induction logs were well suited for low resistivity sandy-shaly formations drilled with water-based mud of relatively high resistivity.

Differences between the interpretation of carbonate and siliciclastic rocks based on matrix parameters were mainly the consequence of mineral composition. In carbonates, calcite, dolomite and shale were adopted as constituents, while in siliciclastic formations the main role was played by quartz and illite.

Total porosities in both formations were similar; average values were about 15%. Effective porosity was more or less similar to the total in carbonates, and distinctly lower in siliciclastic formations. Effective porosity in sandstone formations decreased because of high volumes and dispersed forms of clay minerals in the layer by volume. However, in carbonates, the shaliness was present in the pore space, fractures and matrix.

It was necessary to use different saturation models in shaly sandstones because of the high amount of clay minerals (even up to 60%), compared to carbonate formations where shale volume was between 10–15%.

Particularly important were differences of the saturation type – in the Cuban reservoirs, the pore space was highly saturated with oil while in the Carpathian Foredeep, gas presence was very low.

Error analysis was interesting when assessing the quality of the interpretation. Techlog software presents errors in a separate track (Fig. 12 – last track). It is the sum of differences between measured logs and reconstructed logs divided by standard deviations. The error that occurs is largely dependent on the type of lithology. In the case of carbonate formations, which are more homogeneous, the estimated error is smaller than in thin bed formations or formations with high anisotropy. This is related to the resolution of the tools, which is larger than the thickness of the shale and sand laminas. The error determined for the interpretation of the carbonate formation was small and constant for the entire interval, therefore it was not placed in Figure 11. As can be seen in Figure 12, which shows the results of the interpretation in well A-1, the largest error was calculated for the upper part of the interval, where thin laminas occurred which were slightly saturated with gas. The error occurring in the thin bed formations can be lowered by using high resolution tools which helps to better adjust the interpretation model to real geological conditions. However, the obtained model is a mathematical solution and therefore reducing the error cannot be

a drawback for adjusting the results to laboratory measurements.

## CONCLUSIONS

Comprehensive interpretation of the well logging data was a complex process in which the trial and error method turned out to be both useful and effective. Obtaining the correct results required a lot of geological, petrological and mineralogical information from the literature, core laboratory measurements and mud logging. Also, interpretation outcomes from other wells in the vicinity of the study area were also useful. The most important stage of the interpretation was the construction of a proper model of the matrix constituents and the description of pore fluids. The pre-calculations and preliminary models obtained by using cross-plots were helpful in adopting proper sets of mineral components. In each case, the analysis was performed individually with individually adopted parameters because comprehensive interpretation in different geological environments and lithology required individual approaches. This outcome was finally applied within the applied matrix model, the recognition of shale volume and shale minerals and, finally, to the implementation of adequate saturation equations.

## REFERENCES

Aguilera R., 1980. *Naturally Fractured Reservoir*. Petroleum Publishing Company.

Akhir N.A.M., Gaafar G.R. & Saaid I.M., 2015. Quantification of clay mineral and log response toward reservoir rock properties. [in:] *ICIPEG 2014: Proceedings of the International Conference on Integrated Petroleum Engineering and Geosciences*, Springer, Singapore, 221–231.

Archie G.E., 1942. *The Electrical Resistivity Log as an Aid in Determining Some Reservoirs Characteristics*. Transactions of the AIME, 146, SPE-942054-G, Society of Petroleum Engineers.

Asquith G. & Krygowski D., 2004. *Basic Well Log Analysis*. AAPG Methods in Exploration Series, 16, Oklahoma, USA.

Ballay R.E., Roy R. & Cox E., 2005. *Formation Evaluation: Carbonate versus Sandstone*. Robert Ballay LLC.

Castro O., 1992. *Evaluación de las Formaciones Gaspetroliferas en las UTE Placetas-Camajuani de la región Habana Matanzas, por investigaciones de pozo*. Library of Technological University of Havana, Havana [in Ph.D. Thesis of J.A. Echeverría].

Computing Petrophysical cut off, 2015, [on-line] www.geoloil.com/petroCutoffs.php.htm [access: February 2019].

Crain P., 2002. *Crain's Petrophysical Handbook*. [on-line:] https://www.spec2000.net/00-index.htm [access: February 2019].

Filo M., 2006–2007. Trzciana-Cierpisz-Zaczernie3D – Report of seismic investigations of Geofizyka Kraków Sp. z o.o. Archives of Geofizyka Kraków.

Folk L.R., 1980. *Petrology of Sedimentary Rocks*. Hemphill Publishing Company, Austin, Texas, USA.

Jarzyna J., Bała M. & Zorski T., 1999. *Metody geofizyki otworowej: pomiary i interpretacja*. Uczelniane Wydawnictwa Naukowo-Dydaktyczne AGH, Kraków.

Karnkowski P., 1999. *Oil and Gas Deposits in Poland*. Geosynoptics Society Geos, Krakow.

Klaja J. & Dudek L., 2016. Geological interpretation of spectral gamma ray (SGR) logging in selected boreholes. *Nafta-Gaz*, 72, 1, 3–14.

Log Interpretation Principles and Application, Schlumberger, 1989. [on-line:] https://www.slb.com/resources/publications/books/lipa.aspx [access: February 2019].

López O., Tavarez D., Alberto H., Dominguez R., Prol J., Baños N.S., Tamayo Y., Veiga C., César R.O. & Arriaza G.L., 2012. *Interpretación parcial de la sísmica 3D, área Varadero-Seboruco*. Digital Archives, Oil Research Centre (CEINPET), Havana, Cuba.

López O., Delgado O., Castro O., Blanco S., Morales C. & Tamayo Y., 2015. *Play de Arenas del Oxfordiano (Hipotético)*. Digital Archives. Oil Research Centre (CEINPET), Havana, Cuba.

Montaron B., 2005. *Reinventing Carbonate Petrophysics*. Oilfield Review, Schlumberger.

Moretti I., Tenreyro R., Linares E., Lopez J.G., Letouzey J., Magnier C., Gaumet F., Lecomte J.C., Lopez J.O. & Zimine S., 2003. Petroleum system of the Cuban northwest offshore zone [in:] Bartolini C., Buffler R.T. & Blickwede J. (eds.), *The Circum-Gulf of Mexico and the Caribbean: Hydrocarbon habitats, basin formation, and plate tectonics*, AAPG Memoir, 79, American Association of Petroleum Geologists, 675–696.

Niepsuj M. & Krakowska P., 2012. Analysis and modelling of petrophysical parameters of the Main Dolomite formation on the basis of well logging and seismic data. *Geology, Geophysics & Environment*, 38, 3, 317–327.

Nosal J. & Semyrka R., 2012. Underground $CO_2$ storage – case study of Jastrząbka Stara structure, SE Poland. *Geology, Geophysics & Environment*, 38, 3, 329–338.

Plewa M. & Plewa S., 1992. *Petrofizyka*. Wydawnictwa Geologiczne, Warszawa.

Schön J.H., 2011. *Physical Properties of Rocks – A Workbook*. Handbook of Petroleum Exploration and Production, 8, Elsevier.

Serra O., 1984. *Fundamentals of Well-Log Interpretation: The Acquisition of Logging Data*. Elsevier, Amsterdam – Oxford – New York – Tokyo.

Syrek-Moryc C., 2006. The deposit of natural gas Cierpisz as an important point in the issues concerning the future search in the thin strata of Miocene deposits of the Carpathian Foredeep and potential natural gas resources connected with the deposits. [in:] *Międzynarodowa Konferencja Naukowo-Techniczna Geopetrol 2006 nt. Problemy techniczne i technologiczne pozyskiwania węglowodorów a zrównoważony rozwój gospodarki: Zakopane, 18–21.09.2006*, Prace Instytutu Nafty i Gazu, 137, Instytut Nafty i Gazu, Kraków, 18.

Techlog Online Help, Schlumberger Co., 2015. [on-line:] https://www.software.slb.com/products/techlog/techlog-2015 [access: February 2019].